OPEN ACCESS
Chemistry & Material Sciences Research Journal
Volume 3, Issue 2, P.No. 15-27, March, 2021
DOI: 10.51594/cmsrj.v3i2.216
Fair East Publishers
Journal Homepage: www.fepbl.com/index.php/cmsrj

ANISOTROPIC, SORPTION AND FILTERING PROPERTIES OF THIN-LAYER POLYMER MATERIALS

A.A. Kholmuminov[1], B.M. Matyakubov[1,2,*], T.T. Rakhmonov[2]

[1]Nanotechnology Development Center, National University of Uzbekistan, Tashkent, 100174 Republic of Uzbekistan.
[2]Military Technical Institute of the National Guard of the Republic of Uzbekistan. Tashkent, 100109 Republic of Uzbekistan

*Corresponding Author: B.M. Matyakubov

Article Received: 15-12-20 **Accepted:** 25-02-21 **Published:** 31-03-21

ABSTRACT

The paper presents the results of studies on the production of thin-layer nanofiber non-woven materials based on silk fibroin and acrylonitrile copolymer by the electrospinning method. The dependence of anisotropy characterizing the structural states of the obtained thin-layer polymeric materials on deformation effects, their sorption and filtration properties has been studied. The broad possibility of using nanofiber nonwoven materials as nanofilters and the efficiency of the filtration process of nonwoven materials with an increase in the size of their nanopores are shown.

K**eywords:** Polymer, Silk Fibroin, Acrylonitrile Copolymer, Electrospinning, Isotropic, Anisotropic, Orientation, Nanofiber, Nanomaterial, Formation, Structure, Deformation, Nanofilter.

INTRODUCTION

Thin-layer non-woven functional materials based on polymer are of great importance in production, depending on their composition, molecular and supramolecular structure. They are widely used in various industries as biomedical coatings, fiber nonwovens, nanofilters, sorbents, insulators, laminates and capsules.

The property of shape change due to the influence of external forces of thin polymer materials is the cause of changes in macromolecules in their composition, crystal-amorphous structure, physical state of micro- and nanofibrils, transition from a nonequilibrium isotropic state to an equilibrium anisotropic state (Greiner & Wendorff, 2008; Reneker & Chun, 1996; Nayak & Padhye, 2017)

In recent years, the rapid development of nanotechnology has become a sharp impetus for the creation of thin-layer functional polymer nanomaterials. In such materials, one of the layers serves as the basis of the material, while the other performs a functional task on its surface (He, Guo, & Cui, 2011; Zhou, he, Cui, & Gao, 2011; Koziara, Nijmeijer, & Benes, 2015; Huang, Zhang, Kotaki, & Ramakrishna, 2003; Huang, McMillan, Apkarian, Pourdeyhimi, Conticello, & Chaikof, 2000)

For example, if a nanofiber laminate based on fibroin silk (FS) and acrylonitrile copolymer (Co-AN) is formed, then due to the relatively high degree of flexibility and electrostatic activity of nanofibers (Co-AN), they can be used as substrates. And fibroin due to the relative strength and biological activity due to the amine groups in its composition, they can be used on the surface as a functional biolayer (Kholmuminov, Matyakubov, & Rakhmonov, 2020)

The sequence of the formation of nanofibers from different polymer solutions by the electrospinning method makes it possible to obtain thin-layer nonwoven materials.

Objects and Methods of Research

As a result of the creation of a strong electric field between the die (anode) and a special screen (cathode), using the electrospinning method, polymer nanofibers under the action of a high voltage (U = 1 - 30 kV) intensively evaporate the solvent from the solution stream leaving the die needle. After that, the polymer molecules, stretching orientationally, turn into a nanofiber and hit the surface of the screen, forming randomly laid nonwoven materials in an arbitrary form. In this case, it is important to find the critical value (U_{cr}) of high voltage, bearing in mind the physical and physicochemical index of polymer solutions (Kim, Nam, Lee, & Park, 2003; Shakarova, Begimkulova, & Kholmuminov, 2018).

$$U_{cr} = 4S^2/l^2[ln(2l/r) - 3/2]0{,}117\pi r\alpha_s$$

Here, l – is the length of the spinneret needle and r – is diameter; S – is the distance from the anode to the cathode; α_s – is the surface tension of the polymer solution.

In the general case, if the diameter of the die r = 0.2 - 0.5 mm and with a length of l = 2 - 4 cm, and if voltage is applied to each 1 cm of 1 kV for a distance (at least 20 cm) from the anode to the cathode, concentration C = 3 - 20%, it is determined that it is possible to obtain nanofibers from a polymer mixture. In this case, the regulation of the thickness (d_n) of nanofibers is realized by changing the parameters r, U_{cr}, S, C.

Nanofibers are anisotropic structures with a high orientation factor. With a chaotic arrangement of a thin-layer material on a stationary electrospinning screen, its optical anisotropy has a relatively low index and even forms an isotropic material.

If, instead of a screen, a reel-drum is used, then the nanofibers are laid orientationally folded and formed as a material having a high degree of optically and anisotropic effect (Zhang, Venugopal, & Huang, 2006; Huang, Zhang, Ramakrishna, & Lim, 2004; Amiraliyan, Nouri,

& Kish, 2010; Campoy-Quiles, Nelson, Etchegoin, Bradley, Zhokhavets,Gobsch, & Bubeck, 2008)

In an isotropic nonwoven materials formed by using a stationary screen, the pores between nanofibers change from nanometer to millimeter size, and the thickness of the material will not be the same.

When using a rotary drum-reel, the nanofibers are roughly superdense and form an anisotropic material with high performance, which has almost no pores between them.

In both cases, there are serious problems associated with the porosity of the formed nanofiber materials, and in order to use them, these problems must be eliminated.

To solve this problem, an eccentrically rotational screen is used in the formation of nanofiber one-dimensional nanoporous nonwoven materials (Pagliara, Vitiello, Camposeo, Polini, Cingolani, Scamarcio, & Pisignano, 2011; Ning, Huang, ling, & Lin, 2018; Salmani & Nouri, 2016; Weiwei, Youzhu, Guibo, & Jialin, 2008; Hang, Lu, Bailey, Jimenez-Palomar, Stachewicz, Cortes-Ballesteros, & Barber, 2011)

When using the electrospinning method with an eccentrically rotational screen, a thin-layer nanofiber non-woven material based on fibroin and (Co-AN) is formed.

Its total thickness has a dimension of $d_m \approx 50$ μm, the thickness of the layer of nanofibers (Co-AN) and fibroin nanofibers is, respectively, $d_{Co\text{-}AN} \approx 40$ μm and $d_{FS} \approx 10$ μm (the measurement error is ± 2 μm).

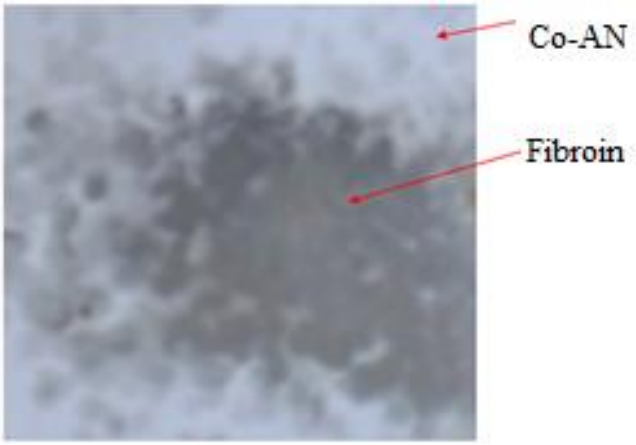

Figure: 1. Micrograph of thin-layer nanofiber non-woven materials based on Co-AN and fibroin

The obtained thin-layer nanofiber nonwoven materials, in the isotropic and anisotropic state due to deformational changes in the transitions, is considered important to study the surface activity (Kholmuminov & Matyaqubov, 2019)

For this, a polarization-optical installation is used, consisting of mechanical and optical parts. In the mechanical part, the sample is stretched vertically with the same rotational frequency. In the optical part, polarization radiation crosses the sample perpendicularly, that is, in the horizontal direction and a polarizing microscope observes the optically anisotropic effect and determines the birefringence index.

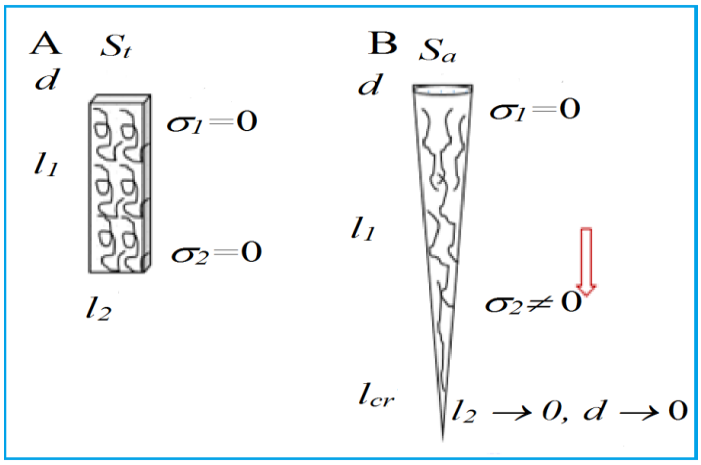

Figure: 2. Schematic diagram of the change in the figure of the sample through deformational tension

Initially, to state A, when the drum-reel does not rotate, there is no mechanical stress at the ends of the sample ($\sigma_1 = \sigma_2 = 0$), while its length (l_1), width (l_2) and thickness (d), in general, the characteristic area $S_t = l_2 \times d$, volume and mass do not change.

After that, in state B, the reel drum rotates with the same frequency (ω) and the condition $\sigma_1 < \sigma_2 \neq 0$ is fulfilled, the belt stretching along its length deformation changes its shape.

When the sample length reaches a certain critical value $l_1 = l_{cr}$, the condition $l_2 \to 0$, $d \to 0$ is satisfied, and a rupture occurs.

The characteristic quadrangular area S_t due to deformation changes turns into a round area $S_a = \pi(d/2)^{0,5}$.

During deformational tension, the sample mass m_t does not change, but due to the compaction of the constituent elements due to deformation-orientational alignment, a decrease in the sample volume V_t is observed.

In the optical part, the sample is inserted perpendicular to the monochromatic radiation, polarized between the polarizer and the analyzer.

Monochromatic radiation, wavelength λ = 560 nm, is isolated with the help of the filter and, being transformed into beams of parallel radiation with the help of lenses, passes through the polaroid, sample, objective, analyzer and eyepiece lying on the same line. The radiation is polarized at the polaroid, i.e. is divided into ordinary and extraordinary radiation.

Due to the deformation stretching of the sample, that is, due to a change in the shape and arrangement of the constituent elements, ordinary radiation is rotated by an angle φ_1 and is observed as an optically anisotropic effect (Fig. 3) (Ayutsede, Gandhi, Sukigara, Micklus, Chen, & Ko, 2005)

By means of a special conical dial where the analyzer is installed, the difference between ordinary and extraordinary radiation is measured. That is, the difference ($\Delta\varphi$) between the optically “black” (φ_o) and “light” (φ_1) backgrounds located in the center of the optical anisotropy. And the thickness (d) of the sample is measured using the eyepiece microscopes.

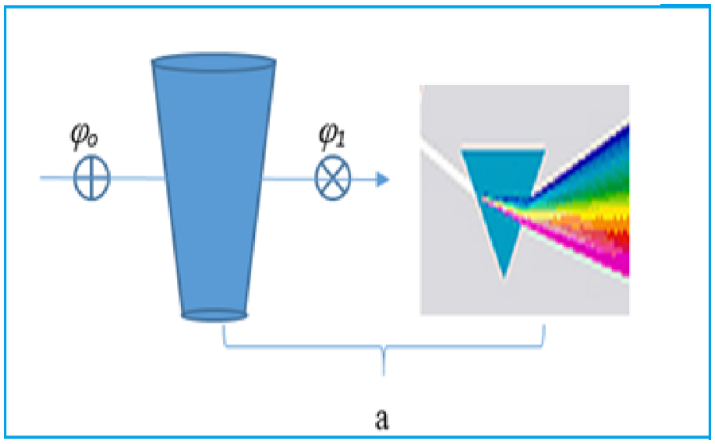

Figure: 3. Schematic diagram of optical anisotropy detection

The thickness of the thin-layer nanofiber nonwoven material is 50 μm (± 2 μm). Polarization-optical radiation passing through it reveals the optical anisotropy of a thin-layer material due to crystallization of macromolecular fibers of fibroin in an orientation order of the highest degree (see Fig. 4) (Campoy-Quiles, Etchegoin, & Bradley, 2005; Xue, Wu, Dai, & Xia, 2019)

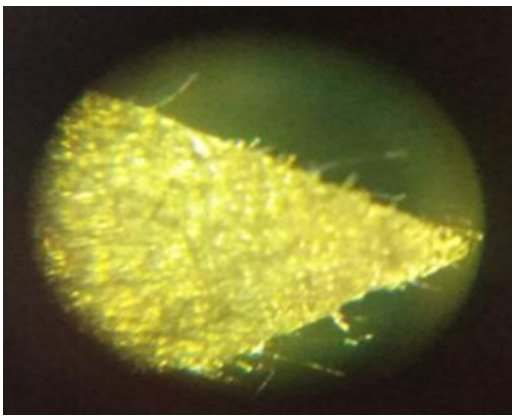

Figure: 4. Polarization optical microscopic image of a thin-layer non-woven material with fibroin fibers

At the same time, two types of birefringence effect are observed in the material based on silk fibroin: the birefringence effect (Δn_{FS}) due to the intrinsic optical anisotropy of fibroin microfibers and the birefringence effect due to the chaotic isotropic arrangement of anisotropic fibroin microfibers on a thin silky nonwoven material.

RESULTS AND DISCUSSION.

It was determined that these values for a specially selected fiber of fibroin are $\Delta n_{FS} = \lambda\Delta\varphi/180d = 560*10^{-9}*65^{o}/180^{o}*50*10^{-6} = 40{,}4*10^{-4}$ and for a thin non-woven material $\Delta n_m = \lambda\Delta\varphi/180d = 560*10^{-9}*10^{o}/180^{o}*50*10^{-6} = 6{,}2*10^{-4}$. Here, the measurement error $\Delta\varphi$ is $\pm 0{,}01^{o}$.

Assuming that the value of the birefringence index of the initial sample $\Delta n_o = \lambda\Delta\varphi_o/180d_o$ and its value during the deformation change $\Delta n_i = \lambda\Delta\varphi_i/180d_i$, one can determine the orientation factor (β) from their ratio, i.e. their anisotropic characteristics are defined as:

$$\beta = [(\Delta n_i - \Delta n_o)/\Delta n_i]^{0,5}$$

With longitudinal and transverse strain tension, the amount of mechanical strength ($\sigma_б$, MPa and $\sigma_к$, MPa) of the sample, and the relative elongation indicators ($\varepsilon_б$, % ва $\varepsilon_к$, %) are determined by the formulas:

$$\sigma_r = F_r/S_o$$

$$\varepsilon_r = (\Delta l_{or}/l_o)100\ \%$$

where F_r - is the tensile stress at break (N); S_o - is the initial cross-section of the sample (mm^2), Δl_{or} is the change in the length of the sample at break (mm); l_o - initial sample length (mm).

The experiments were carried out on the basis of non-woven materials obtained in the mode 2 rpm and having a thickness of 50 μm (± 2 μm).

And also the mechanical $A_м = \sigma_c/\sigma_к$ and optical anisotropies $A_o = \beta_c/\beta_к$ of the material are determined. The results are shown in Table-1.

Table 1: Indicators at Deformation Attraction of The Sample

ω, rpm	d, μm	Sample breakage performance						A_m	A_o
		With continued			With transverse				
		σ_c, MPa	ε_c, %	β_c	$\sigma_к$, MPa	$\varepsilon_к$, %	$\beta_к$		
2,0	50	68	539	0,91	64	530	0,82	1,10	1,12
3,5	41	76	390	0,94	42	294	0,55	1,81	1,72
4,5	36	81	335	0,96	35	214	0,43	2,31	2,24

When analyzing the dependence of the relative elongation ($\varepsilon_б$) on the attractive stress ($\sigma_б$). Those, during the graphic analysis, three characteristic deformation-changing areas were identified. If the effects of the 2 - and 3 - regions are explained with the realization of the volumetric strain-induced tension of the material, then the internal molecular-megmental changes in the material, i.e., the deformation-orientational incorporation of amorphous macromolecules, explains the transition to the anisotropic state due to the relatively low consumption of tensile stress.

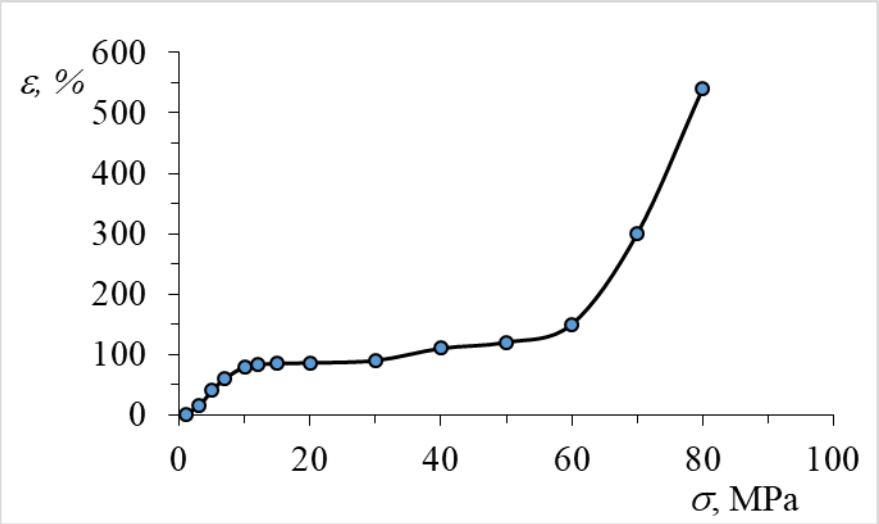

Figure: 5. Dependence relative deformation elongation on mechanical stress

Using the results of the experiment carried out with a deformation change ($\sigma_б$) through the polarization-optical system, the dependences of the orientation factor *(β)* on the attraction stress were obtained.

In Fig. 6, one can observe three characteristic regions that differ from each other in the values of optical anisotropy and orientation factor.

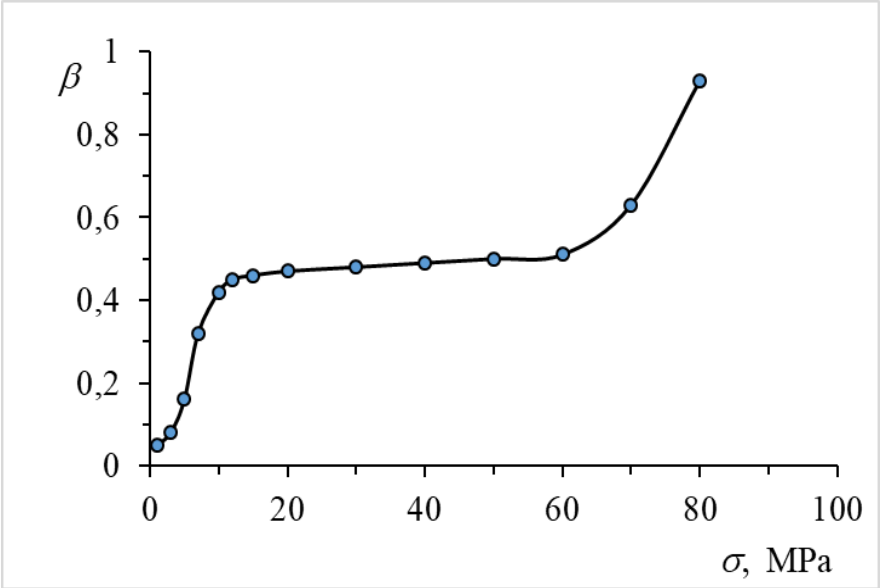

Fig. 6. Dependence of orientation factor on attraction strength

Micrographs representing the change in optical anisotropy of thin-layer non-woven microfiber and nanofiber fibroin materials are shown in Figure-7.

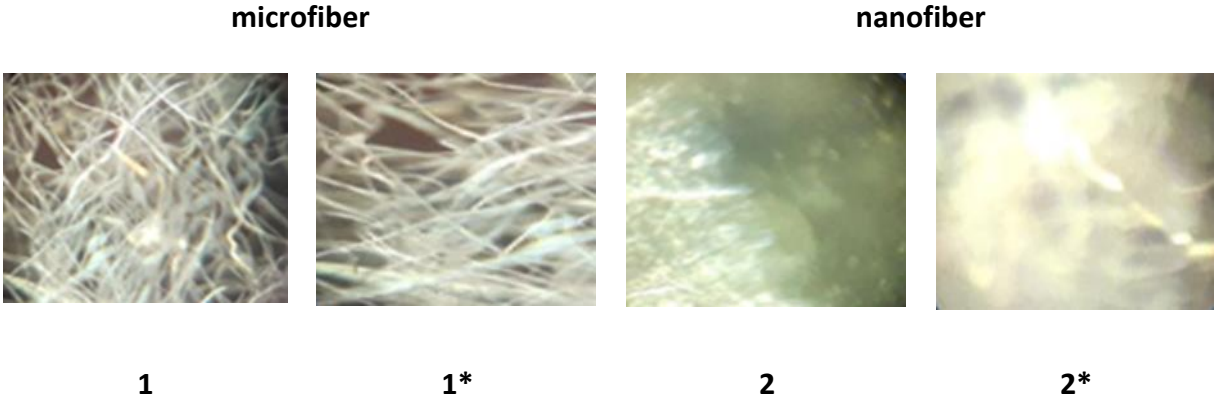

Figure-7. Micrographs of micro- and nano-fiber fibroin materials:
1 - ε = 0%; 1* - ε = 100%; 2 - ε = 0%; 2* - ε = 100%

After an increase in the relative elongation from ε > 100 % , a rupture effect is observed on microfiber and nanofiber materials. But the orientation factor *(β)* is calculated based on the values *(Δφ)* measured in the range 0 > ε > 100 %. Based on the results, a graph is plotted (see Figure 8) orientation factor *(β)* versus elongation (ε).

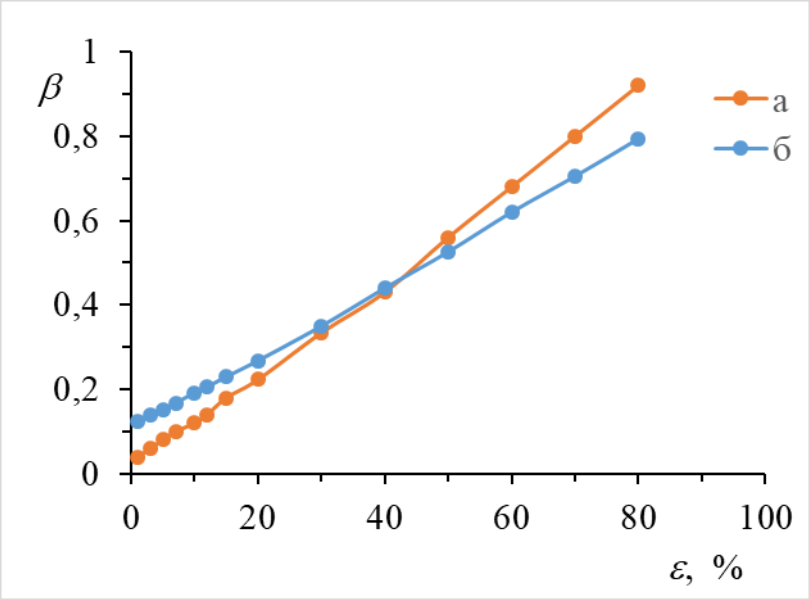

Figure: 8. Dependence of the orientation factor on the relative elongation:
a - material from microfiber fibroin; b - material from nanofiber fibroin

The graphs are straight-line and represent the proportional increase in elongation versus optical orientation factor. Those. from optical anisotropy.

- material with microfibers of fibroin - $\beta = k\varepsilon = 0{,}0112\varepsilon$
- material with nanofibers of fibroin - $\beta = k\varepsilon = 0{,}0084\varepsilon$

This coefficient and the linear dependence of the deformation change of a thin-layer material based on fibroin on optical anisotropy make it possible to estimate the deformation state of a thin-layer material through optical anisotropy (Li, Li, Zheng, Luo, Liu, Wu, & Kaplan, 2016). *Sorption.* In the second table and in Fig. 9 shows the results of a comparative sorption experiment when water and ethanol were used as sorbate.

Table 2: Results of Sorption of Thin-Layer Nanomaterials

Relative humidity, P/P_o, %	Thin-layer nanomaterial (Co-AN:FS = 70:30)	
	Ethanol	Water
	Sorption degree, $a = (x/м)$, %	
10	0,10	0,30
30	0,30	0,60
50	0,40	0,90
65	0,60	1,00
80	0,80	1,30
90	1,20	2,10
100	1,60	3,90

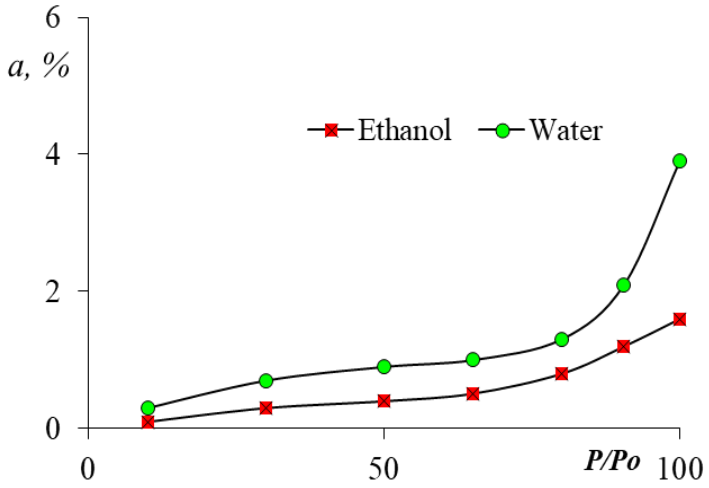

Fig. 9. Sorption of thin-layer nanomaterials of water and ethanol vapor

From the results obtained, it can be seen that the thin-layer nanomaterial sorbs relatively well, i.e. absorbs water vapor. The reason for this is the hydrophilicity of the functional amine, hodroxyl, and carbixyl groups of the biopolymer fibroin, i.e. their active interaction with water molecules.

The sorption process was also realized on ethanol, but the hydrophobicity of proteins, which is characteristic of precipitants, was revealed here (Elkasaby, Utkarsh, Syed, Rizvi, Mohany, & Pop-Iliev, 2020)

Table 3 shows the values of the physical parameters of layered nanomaterials: the relative surface of the nanofiber ($S_{отн}$) the total volume of existing nanopores (W_o) and the average radius of the pore-capillaries ($r_к$).

Table 3: Sorption Indicators of Thin-Layer Nanomaterials

Indicators	Thin-layer nanomaterial (Co-AN:FS = 70:30)	
	Ethanol	Water
$X_м$, *г/г*	0,0039	0,0052
$S_{уд}$, $м^2/г$	12,91	18,33
W_o, $см^3/г$	0,020	0,039
$r_к$, *Å*	38,41	42,55

As noted in the above, the number of sorption parameters in water is relatively small, this is due to the peculiarities of revealing in the sorption process the hydrophilic nature of fibroin and the hydrophobicity of the acrylonitrile copolymer. From the data determined for both sorbates, the values of porous capillary radii are close to each other. This circumstance makes it possible to use layered materials not only as bioactive materials, but also as a nanofilter.

Filtration. To study the filtration ability of nanofiber nonwoven materials based on fibroin and acrylonitrile copolymer, we used a device for purifying the composition of almost non-swellable liquids, assembled according to the scheme shown in Fig. 10.

By choosing such special fluids, elimination of changes under deformation effect and swelling of nanopores were achieved. These experiments were carried out in a centrifuge on machine oil, in which the fibroin and acrylonitrile nanofibers do not swell (Fang, Niu, Lin, & Wang, 2008).

For the experiments, we selected nanofiber nonwoven materials with a thickness of d_m = 0.5 mm and pore sizes of 50, 100, 300 nm, and all of them are individually fixed into the device.

Waste machine oil taken m_o = 100 ml was poured onto a filtration device, i.e. onto the nanofilter and measured the time *(t)* of complete passage through it.

It was observed how this waste machine oil passed through the nanofilter becomes transparent and the mass (m_i) of the filtered oil collected in a special vessel was measured.

The ability of the nanofilter to retain particles in the composition of engine oil was determined, i.e., the filtration index according to the formula $m_{us} = (m_i / m_o) * 100\%$.

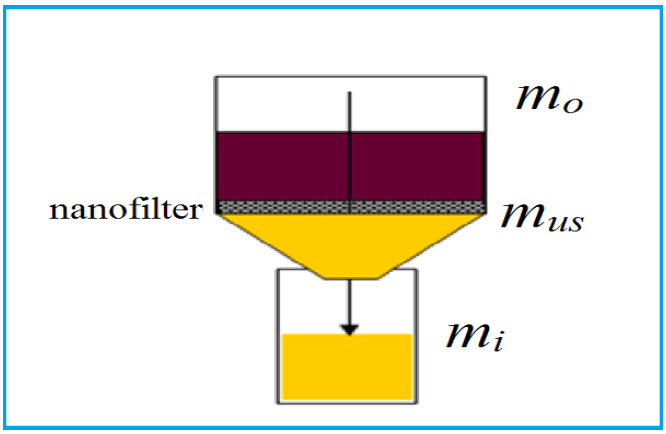

Figure: 10. Nanofilter Device

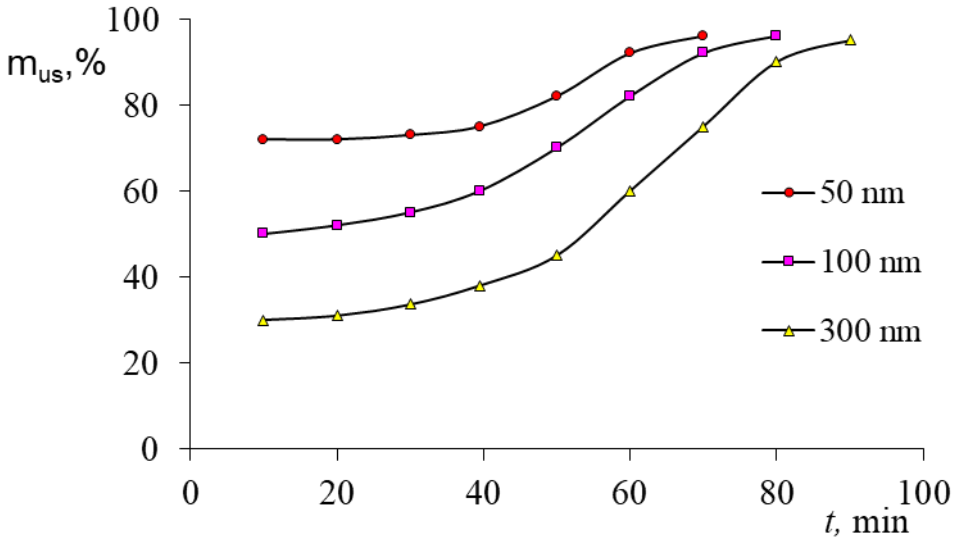

Figure: 11. Dependence of the Filtration Index On Time

The experiment obtained results similar to the results obtained for fibroin and Co-AN. Therefore, in the discussion we will restrict ourselves to the results obtained for Co-AN.

An increase in the retention index of a nanofilter particle in the composition of engine oil has been substantiated over time, and a shift in the graphs of the dependences of a decrease in the values of nanopores towards high $\boldsymbol{m_{us}}$ and small *m* sections is shown.

The observation of such a process is associated, firstly, with a direct change in the size of the material, and secondly, after 40 - 45 min of the filtration process, a relatively intense increase in the amount of ***m*** is revealed, and when it is exceeded from 95%, a slowdown of this growth is observed.

CONCLUSION

The results obtained showed the possibility of forming thin-layer materials based on silk fibroin and acrylonitrile copolymer, their peculiar characteristics in a hydrophilic and hydrophobic environment. This fact provides evidence of the use of layered materials not only as bioactive materials, but also to use them as nanofilters. The high possibilities of using nanofiber nonwoven materials as nanofilters and an increase in filtration efficiency with an increase in the size of nanopore nonwoven materials are shown.

References

Amiraliyan, N., Nouri, M., & Kish, M. H. (2010). Structural characterization and mechanical properties of electrospun silk fibroin nanofiber mats. *Polymer Science Series A*, *52*(4), 407-412.

Ayutsede, J., Gandhi, M., Sukigara, S., Micklus, M., Chen, H. E., & Ko, F. (2005). Regeneration of Bombyx mori silk by electrospinning. Part 3: characterization of electrospun nonwoven mat. *Polymer*, *46*(5), 1625-1634.

Campoy-Quiles, M., Etchegoin, P. G., & Bradley, D. D. C. (2005). On the optical anisotropy of conjugated polymer thin films. *Physical Review B*, *72*(4), 045209.

Campoy-Quiles, M., Heliotis, G., Xia, R., Ariu, M., Pintani, M., Etchegoin, P., & Bradley, D. D. (2005). Ellipsometric characterization of the optical constants of polyfluorene gain media. *Advanced Functional Materials, 15*(6), 925-933.

Campoy-Quiles, M., Nelson, J., Etchegoin, P. G., Bradley, D. D. C., Zhokhavets, V., Gobsch, G., ... & Bubeck, C. (2008). On the determination of anisotropy in polymer thin films: A comparative study of optical techniques. *Physica Status Solidi c*, *5*(5), 1270-1273.

Elkasaby, M. A., Utkarsh, Syed, N. A., Rizvi, G., Mohany, A., & Pop-Iliev, R. (2020, January). Evaluation of electro-spun polymeric nanofibers for sound absorption applications. In *AIP Conference Proceedings* (Vol. 2205, No. 1, p. 020042). AIP Publishing LLC.

Fang, J., Niu, H., Lin, T., & Wang, X. (2008). Applications of electrospun nanofibers. *Chinese Science Bulletin*, *53*(15), 2265-2286.

Greiner, A., & Wendorff, J. H. (2008). Functional self-assembled nanofibers by electrospinning. *Self-Assembled Nanomaterials I*, 107-171.

Hang, F., Lu, D., Bailey, R. J., Jimenez-Palomar, I., Stachewicz, U., Cortes-Ballesteros, B., ... & Barber, A. H. (2011). In situ tensile testing of nanofibers by combining atomic force microscopy and scanning electron microscopy. *Nanotechnology*, *22*(36), 365708.

He, J., Guo, N., & Cui, S. (2011). Structure and Mechanical Properties of Electrospun Tussah Silk Fibroin Nanofibres: Variations in Processing Parameters. *Iranian Polymer Journal, 20*(9), 713-724.

Huang, L., McMillan, R. A., Apkarian, R. P., Pourdeyhimi, B., Conticello, V. P., & Chaikof, E. L. (2000). Generation of synthetic elastin-mimetic small diameter fibers and fiber networks. *Macromolecules*, *33*(8), 2989-2997.

Huang, Z. M., Zhang, Y. Z., Kotaki, M., & Ramakrishna, S. (2003). A review on polymer nanofibers by electrospinning and their applications in nanocomposites. *Composites Science and Technology*, *63*(15), 2223-2253.

Huang, Z. M., Zhang, Y. Z., Ramakrishna, S., & Lim, C. T. (2004). Electrospinning and mechanical characterization of gelatin nanofibers. *Polymer*, *45*(15), 5361-5368.

Kholmuminov, A. A., & Matyaqubov, B. M. (2019). Nano-Fiber Nonwoven Materials of Polymers with Surface-Active Properties. *Journal of Scientific and Engineering Research*, *6*(11), 232-235.

Kholmuminov, A. A., Matyakubov, B. M., & Rakhmonov, T. T. (2020). Optical anisotropic properties of nanofiber polymer materials. *ISJ Theoretical & Applied Sciences, 02*(82), 249-253.

Kim, S. H., Nam, Y. S., Lee, T. S., & Park, W. H. (2003). Silk fibroin nanofiber. Electrospinning, properties, and structure. *Polymer Journal*, *35*(2), 185-190.

Koziara, B. T., Nijmeijer, K., & Benes, N. E. (2015). Optical anisotropy, molecular orientations, and internal stresses in thin sulfonated poly (ether ether ketone) films. *Journal of Materials Science*, *50*(8), 3031-3040.

Li, G., Li, F., Zheng, Z., Luo, T., Liu, J., Wu, J., ... & Kaplan, D. L. (2016). Silk microfiber-reinforced silk composite scaffolds: fabrication, mechanical properties, and cytocompatibility. *Journal of materials science*, *51*(6), 3025-3035.

Nayak, R., & Padhye, R. (2017). Nano fibres by electro spinning, properties and applications. *Journal of Textile Engineering & Fashion Technology*, *2*(5), 486-497.

Ning, W., Huang, J., Ling, X., & Lin, H. (2018, October). Modification of electrospun silk fibroin nanofiber mats: using an EDC/NHS ethanol solvent. In *IOP Conference Series: Materials Science and Engineering* (Vol. 423, No. 1, p. 012068). IOP Publishing.

Pagliara, S., Vitiello, M. S., Camposeo, A., Polini, A., Cingolani, R., Scamarcio, G., & Pisignano, D. (2011). Optical anisotropy in single light-emitting polymer nanofibers. *The Journal of Physical Chemistry C*, *115*(42), 20399-20405.

Reneker, D. H., & Chun, I. (1996). Nanometre diameter fibres of polymer, produced by electrospinning. *Nanotechnology*, *7*(3), 216.

Salmani, L., & Nouri, M. (2016). Electrospun silk fibroin nanofibers with improved surface texture. *Journal of textiles and polymers*, *4*(2), 75–82

Shakarova, D. S., Begimkulova, C. K., & Kholmuminov, A. A. (2018). Surface-Active Properties of nanofibers on the basis of Fibroin Silk and Copolymer Acrylonitrile. *International Journal of Advanced Scientific and Technical*, (8), 62-67.

Weiwei, B., Youzhu, Z., Guibo, Y., & Jialin, W. (2008). The structure and property of the electrospinning silk fibroin/gelatin blend nanofibers. *e-Polymers*, *8*(1).

Xue, J., Wu, T., Dai, Y., & Xia, Y. (2019). Electrospinning and electrospun nanofibers: Methods, materials, and applications. *Chemical Reviews*, *119*(8), 5298-5415.

Zhang, Y.Z., Venugopal, J., & Huang, Z.M. (2006). Crosslinking of the electrospun gelatin nanofibers. *Polymer*, *47*(8), 2911-2917.

Zhou, W., He, J., Cui, S., & Gao, W. (2011). Preparation of electrospun silk fibroin/Cellulose Acetate blend nanofibers and their applications to heavy metal ions adsorption. *Fibers and Polymers*, *12*(4), 431-437.